Asociación Argentina
de Mecánica Computacional

Mecánica Computacional Vol XXXII, págs. 439-452 (artículo completo)
Carlos G. García Garino, Aníbal E. Mirasso, Mario A. Storti, Miguel E. Tornello (Eds.)
Mendoza, Argentina, 19-22 Noviembre 2013

MICROMECHANICAL APPROACH TO POROELASTIC PROPERTIES OF CRACKED ROCKS

Giordano Lorenci, Eduardo Bittencourt and Samir Maghous

Department of Civil Engineering, Federal University of Rio Grande do Sul, Av. Osvaldo Aranha, 99, 90035-190 Porto Alegre-RS, samir.maghous@ufrgs.br, http://www.engcivil.ufrgs.br

Keywords: Jointed rock, poroelasticity, micromechanics.

Abstract. The formulation of macroscopic poroelastic behavior of a jointed rock is investigated within the framework of a micro-macro approach. Particular emphasis is given to the situation of small joints (i.e., cracks) with pressurized saturating fluid. The joints are modeled as interfaces and their behavior is modeled by means of generalized poroelastic state equations. Starting from Hill's lemma extended for a jointed medium and extending the concept of strain concentration to relate the joint displacement jump to macroscopic strain, the overall poroelastic constitutive equations for the jointed rock are formulated. The analysis emphasizes the main differences and similarities of the resulting behavior with respect to that characterizing ordinary porous media. It is shown that, unlike ordinary porous media, conditions on the poroelastic parameters of joints are required for the macroscopic drained stiffness to entirely define the poroelastic behavior. This is achieved, for instance, if the joint network is characterized by a unique Biot coefficient. A micromechanical scheme is then applied to derive analytically the homogenized poroelastic properties in two particular situations: a rock with a network of parallel cracks and the situation of isotropically distributed cracks. and Extension of the analysis to non-linear poroelasticity is finally outlined. Validation of the model is made by comparison with finite element solutions based on the cohesive model for the joints.

Copyright © 2013 Asociación Argentina de Mecánica Computacional http://www.amcaonline.org.ar

1 INTRODUCTION

It is well-known from observations made at different scales that rock masses generally exhibit discontinuity surfaces of various sizes and orientations, commonly referred to as joints. Since joints represent surfaces of weakness along which sliding can occur and preferential channels for fluid flow, their presence is a fundamental weak component for stability and safety of many rock engineering structures, such as dam foundations, underground caverns, oil wells or toxic waste storage facilities. A comprehensive modeling of a rock mass behavior should thus incorporate a reliable description of the hydromechanical coupling that governs the joint deformation.

Strength, deformation and permeability coupling of rock joints have been widely investigated during the previous decades, leading to numerous experimental works and models. Among the pioneering works, one may quote the contributions due to Goodman (1976) and Bandis et al. (1983). Representative references include references (Barton et al., 1985; Ng and Small, 1997; Nguyen and Selvadurai, 1998; Olsson and Barton, 2001; Indraratna and Ranjith, 2001; Boulon et al., 2002; Bart et al., 2004), to cite a few.

Most of the hydromechanical models have, however, focused on the connection between the joint aperture due to applied stresses and the permeability. The effect of fluid pressure on joint deformation have been either neglected or not properly accounted for. Few models have addressed the fully hydromechanical coupling in rock joints (Ng and Small, 1997; Bart et al., 2004; Maghous et al., 2013).

Conceived as a potential alternative to the discrete methods in which the individual joints and the rock matrix are handled separately, the homogenization approach adopts a continuum point view for the formulation of the constitutive behavior of the jointed rock material regarded as a homogenized medium. In this context, a recent paper by Maghous et al. (2013) proposed a general micromechanics-based approach to poroelastic behavior of a jointed rock. In this context, the purpose of this contribution is to extend the formulation to the specific case of parallel of randomly distributed short joints. Emphasis shall be given to derive closed-form expressions for the tensor of homogenized drained moduli, as well as for the effective Biot tensor and modulus. A primary objective of the analysis is to highlight the effect of fluid pressure in the interstitial space of rock short joints on the overall poroelastic properties of the rock mass. The accuracy of the micromechanical prediction is assessed by comparison in a simplified two-dimensional setting with finite element solutions based on the cohesive model. It is convenient to emphasize that, in contrast to the classical model of cracks in which no stresses are transferred across the cracks, the joints are in fact fractures that are able to transfer normal as well as tangential stresses.

Copyright © 2013 Asociación Argentina de Mecánica Computacional http://www.amcaonline.org.ar

2 MICROMECHANICS

Let Ω denote the representative elementary volume (REV) of a homogeneous rock matrix cut by a discrete distribution of short joints $\omega = \bigcup_i \omega_i$. Adjective 'short' refers to joints with small extension when compared to the size of the REV. It is emphasized short joints are in fact microfractures (or microcrack) that are able to transfer stresses. It is also noted that the concept of REV implies the scale separation between its characteristic length and those of joints, namely the size of short joints.

The rock matrix fills the domain $\Omega \setminus \omega$, where symbol $\setminus$ stands for the set difference. Note that strains and stresses within the rock medium are defined on the rock matrix domain $\Omega \setminus \omega$ only, and not on the whole REV. Throughout the paper, symbol $\langle . \rangle$ denotes the volume average over the rock matrix:

$$\langle . \rangle = \frac{1}{|\Omega_0|} \int_{\Omega \setminus \omega} . \; dV \tag{1}$$

2.1 Hill's lemma for the jointed rock

The loading applied to the REV is defined by homogeneous strain type boundary conditions on the boundary $\partial\Omega$:

$$\underline{\xi}(\underline{x}) = \underline{\underline{E}} \cdot \underline{x} \quad \forall \underline{x} \in \partial\Omega \tag{2}$$

where $\underline{\underline{E}}$ represents the macroscopic strain. Hill's lemma reads in the situation of a jointed medium (e.g., Maghous et al., 2008)

$$\langle \underline{\underline{\sigma}} \rangle : \underline{\underline{E}} = \langle \underline{\underline{\sigma}} : \underline{\underline{\varepsilon}} \rangle + \frac{1}{|\Omega_0|} \int_{\omega} \underline{T} \cdot [\underline{\xi}] \; dS \tag{3}$$

for any statically admissible stress fields $\underline{\underline{\sigma}}$ and any kinematically admissible displacement field $\underline{\xi}$. Tensor $\underline{\underline{\varepsilon}}$ represents the linearized strain associated with displacement $\underline{\xi}$ and $[\underline{\xi}]$ is the displacement jump at the joint interface. In the above equation, $\underline{T}$ is the stress vector acting upon the joint.

The strain average rule relating the macroscopic strain to the local strains writes

$$\underline{\underline{E}} = \langle \underline{\underline{\varepsilon}} \rangle + \frac{1}{|\Omega_0|} \int_{\omega} [\underline{\xi}] \overset{s}{\otimes} \underline{n} \; dS \tag{4}$$

where $\underline{n} = \underline{n}_i$ along ω_i and symbol $\overset{s}{\otimes}$ stands for the symmetric part of dyadic product: $\left(\underline{u} \overset{s}{\otimes} \underline{v} \right)_{ij} = (u_i v_j + v_i u_j)/2$. Identity (4) physically means that the macroscopic strain $\underline{\underline{E}}$ is

Copyright © 2013 Asociación Argentina de Mecánica Computacional http://www.amcaonline.org.ar

the sum of two contributions, namely that of rock matrix strains and that of displacement jump along the joints.

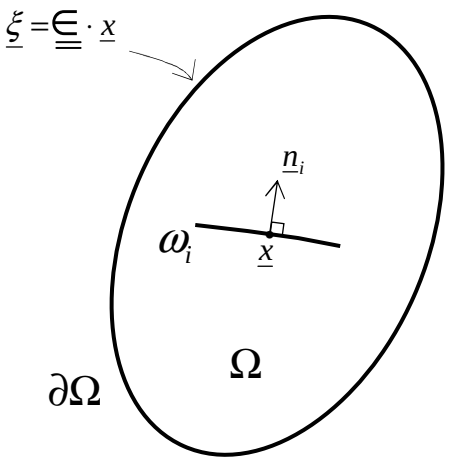

Figure 1: REV of a jointed rock and loading conditions.

2.2 Formulation of the poroelastic state equations

We consider the situation where the connected joint network is saturated by a fluid at pressure p, which is assumed to be uniform in the REV. The rock matrix is assumed to be linearly elastic with fourth-order stiffness tensor $\mathbb{C}^s$: $\underline{\underline{\sigma}} = \mathbb{C}^s : \underline{\underline{\varepsilon}}$ in $\Omega \setminus \omega$. A poroelastic formulation is adopted for the behavior of joints in order to account for the effect of the fluid pressure on the relationship between the stress vector acting on the joint and the corresponding relative displacement. The poroelastic state equations for the joints are written in the following form (Bart et al., 2004; Maghous et al., 2013)

$$\begin{cases} \underline{T} = \underline{\underline{\sigma}} \cdot \underline{n} = \underline{\underline{k}} \cdot [\underline{\xi}] + \underline{T}^p \\ \varphi = \dfrac{p}{m} + \alpha\, [\underline{\xi}] \cdot \underline{n} \end{cases} \quad \text{along } \omega = \bigcup_i \omega_i \quad (\text{with } \underline{n} = \underline{n}_i \text{ along } \omega_i) \tag{5}$$

where

$$\underline{\underline{k}} = \underline{\underline{k}}^i \;, \quad \alpha = \alpha_i \;, \quad m = m_i \;, \quad \underline{T}^p = -\alpha_i\, p\, \underline{n}_i \quad \text{along } \omega_i \tag{6}$$

where $\underline{\underline{k}}^i$ is the stiffness of joint ω_i, relating the stress vector to the displacement jump in drained conditions $p = 0$. Scalar α_i has the significance of a Biot coefficient for the joint ω_i modeled as a generalized porous medium. This means that the displacement jump $[\underline{\xi}]$ which represents the joint deformation is controlled by the effective stress vector $\underline{T} + \alpha p\, \underline{n}$. As regards the second state equation in (5) of the joint, it relates the joint pore change per unit joint surface φ to the fluid pressure p and the joint displacement jump $[\underline{\xi}]$. Scalar m_i

Copyright © 2013 Asociación Argentina de Mecánica Computacional http://www.amcaonline.org.ar

represents the Biot modulus for joint ω_i. Physical interpretation as well as identification procedures of the above parameters from appropriate laboratory tests are outlined in Bart et al. (2004).

The loading is now characterized by two parameters, namely the macroscopic strain $\underline{\underline{E}}$ and the fluid pressure p. The solution in $\Omega \setminus \omega$ to this problem defined by the loading mode $\left(\underline{\underline{E}}\ ,\ p\right)$ and denoted by (P), is defined by the stress field $\underline{\underline{\sigma}}$ and the displacement field $\underline{\xi}$ that are related by the state equations of the medium constituents $\underline{\underline{\sigma}} = \mathbb{C}^s : \underline{\underline{\varepsilon}}$ in $\Omega \setminus \omega$ and (5). Due to the linearity of the material behavior, the superposition principle can be used to decompose problem (P) into two elementary problems (P1) and (P2) respectively defined by the loadings $\left(\underline{\underline{E}}\ ,\ p=0\right)$ and $\left(\underline{\underline{E}}=0\ ,\ p\right)$ as shown in Figure 2. (P1) corresponds to the dry case analyzed in section **3**, whereas (P2) corresponds to pressurized joint network and prevented macroscopic strain.

Let us designate by $\underline{\xi}_i$, $\underline{\underline{\varepsilon}}_i$ and $\underline{\underline{\sigma}}_i$ the displacement, strain and stress fields in the REV corresponding to problem (Pi) for $i \in \{1,2\}$. The fields solution to problem (P) can simply be obtained as $\underline{\xi} = \underline{\xi}_1 + \underline{\xi}_2$, $\underline{\underline{\varepsilon}} = \underline{\underline{\varepsilon}}_1 + \underline{\underline{\varepsilon}}_2$ and $\underline{\underline{\sigma}} = \underline{\underline{\sigma}}_1 + \underline{\underline{\sigma}}_2$.

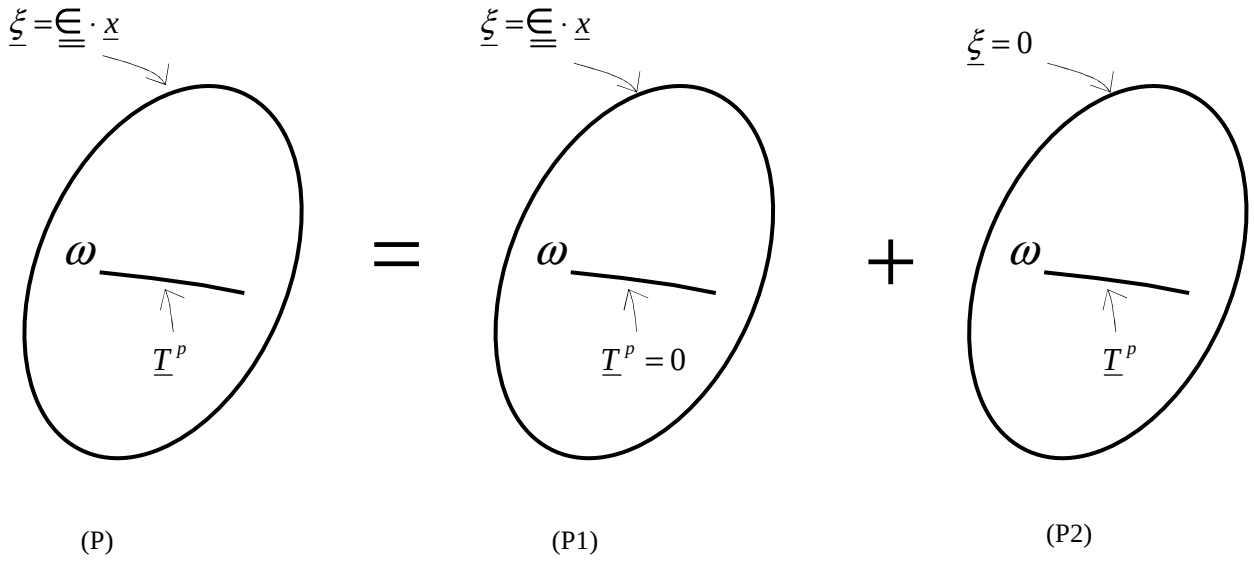

Figure 2: Decomposition of problem (P) into two elementary problems (P1) and (P2).

In problem (P1) corresponding to the dry case, the displacement in the rock matrix is related to the macroscopic strain through the fourth-order tensor $\mathbb{A}$ classically referred to as strain concentration tensor: $\underline{\xi}_1(\underline{x}) = \mathbb{A}(\underline{x}) : \underline{\underline{E}}$. Similarly, we define by anticipation the 2nd-order tensor $\underline{\underline{a}}^n$, which represents the concentration tensor for the normal displacement jump, by

Copyright © 2013 Asociación Argentina de Mecánica Computacional http://www.amcaonline.org.ar

$$[\underline{\xi}_1]\cdot\underline{n}=\underline{\underline{a}}^n:\underline{\underline{\underline{\in}}} \quad \text{along } \omega \tag{7}$$

A classical reasoning in linear elastic homogenization (Zaoui, 2002) shows that

$$\underline{\underline{\Sigma}}_1=\langle\,\underline{\underline{\sigma}}_1\,\rangle=\mathbb{C}^{\text{hom}}:\underline{\underline{\underline{\in}}} \qquad \textit{with} \qquad \mathbb{C}^{\text{hom}}=\langle\,\mathbb{c}^s:\mathbb{A}\,\rangle \tag{8}$$

$\mathbb{C}^{\text{hom}}$ is the elastic tensor of effective drained moduli.

In problem (P2), $\underline{\underline{\Sigma}}_2=\langle\,\underline{\underline{\sigma}}_2\,\rangle$ represents the macroscopic stress associated with joint interstitial fluid pressure p which is required to prevent the appearance of any macroscopic strain. Evaluation $\underline{\underline{\Sigma}}_2$ stems from ther application of Hill's lemma (3) successively to the couples $\left(\underline{\underline{\sigma}}'=\underline{\underline{\sigma}}_2\,,\ \underline{\xi}'=\underline{\xi}_1\right)$ and $\left(\underline{\underline{\sigma}}'=\underline{\underline{\sigma}}_1\,,\ \underline{\xi}'=\underline{\xi}_2\right)$. It is readily obtained after some mathematical manipulations (see Maghous et al., 2013):

$$\underline{\underline{\Sigma}}_2=-\,p\,\underline{\underline{B}} \qquad \textit{with} \quad \underline{\underline{B}}=\frac{1}{|\Omega|}\int_\omega \alpha\,\underline{\underline{a}}^n\ dS \tag{9}$$

The first macroscopic state equation results from superposition of (8) and (9)

$$\underline{\underline{\Sigma}}=\underline{\underline{\Sigma}}_1+\underline{\underline{\Sigma}}_2=\mathbb{C}^{\text{hom}}:\underline{\underline{\underline{\in}}}-p\,\underline{\underline{B}} \tag{10}$$

Similarly to ordinary porous media, the macroscopic strain $\underline{\underline{\underline{\in}}}$ is controlled in poroelasticity by an effective Biot stress $\underline{\underline{\Sigma}}+p\,\underline{\underline{B}}$. The tensor $\underline{\underline{B}}$ defined in Eq. (9) can be interpreted as the tensor of Biot coefficients for the jointed medium. The anisotropy introduced by the joint orientation is captured through that of the normal concentration tensor $\underline{\underline{a}}^n$.

For an ordinary porous medium, the classical relationship $\underline{\underline{B}}=\underline{\underline{1}}:\left(\mathbb{I}-(1-\phi)\,\mathbb{c}^{s\,-1}:\mathbb{C}^{\text{hom}}\right)$ where ϕ is the porosity of the medium (Dormieux et al., 2006), shows that the macroscopic Biot tensor is entirely defined once the macroscopic tensor $\mathbb{C}^{\text{hom}}$ of drained elastic moduli is determined.

Regarding the jointed medium, it follows from (3), (7) and (8) that

$$\frac{1}{|\Omega|}\int_\omega \underline{\underline{a}}^n\ dS=\underline{\underline{1}}:\left(\mathbb{I}-\langle\,\mathbb{A}\,\rangle\right)=\underline{\underline{1}}:\left(\mathbb{I}-\mathbb{c}^{s\,-1}:\mathbb{C}^{\text{hom}}\right) \tag{11}$$

Assuming in what follows that all the joints have the same Biot coefficient, i.e. $\forall i\ \ \alpha_i=\alpha$,

Copyright © 2013 Asociación Argentina de Mecánica Computacional http://www.amcaonline.org.ar

introducing definition (9) of tensor into the above equation provides the following identity

$$\underline{\underline{B}} = \alpha \, \underline{\underline{1}} : \left(\mathbb{I} - \mathbb{c}^{s\,-1} : \mathbb{C}^{\hom} \right) \tag{12}$$

which extends to the case of a jointed medium the classical relationship relating the tensor of Biot coefficients to the elastic tensors of the porous medium and solid matrix.

The complete formulation of the overall poroelastic behavior for the jointed medium is achieved by providing the second macroscopic state equation. The second state equation for the macroscopic poroelastic behavior classically relates the pore volume change to the fluid pressure p and the macroscopic strain $\underline{\underline{\in}}$. In the considered case, the pore volume change is exclusively due to the joint volume change. The lagrangian porosity change is therefore defined as:

$$\Phi = \frac{1}{|\Omega|} \int_{\omega} \varphi \; dS = \frac{1}{|\Omega|} \int_{\omega} \left(\frac{p}{m} + \alpha \, [\underline{\xi}] \cdot \underline{n} \right) \; dS \tag{13}$$

where the second state equation in (5) has been used.

Referring to the decomposition $\underline{\xi} = \underline{\xi}_1 + \underline{\xi}_2$, it is shown in Maghous et al. (2013) that the second state equation reads

$$\Phi = \frac{p}{M} + \underline{\underline{B}} : \underline{\underline{\in}} \tag{14}$$

where the macroscopic Biot modulus M is given by

$$\frac{1}{M} = \sum_i S_i \frac{1}{m_i} + \alpha \, \underline{\underline{1}} : \left(\mathbb{c}^{s} \right)^{-1} : \underline{\underline{B}} \tag{15}$$

$S_i = \frac{1}{|\Omega|} \int_{\omega_i} dS$ being the specific area of joint ω_i.

Relationships (12) and (15) show that the overall properties M and $\underline{\underline{B}}$ are entirely known once the macroscopic tensor $\mathbb{C}^{\hom}$ of drained elastic moduli is determined. These relationships extend to the situation of jointed rock medium the classical relationships providing the Biot tensor and Biot modulus as functions of solid matrix elasticity $\mathbb{c}^{s}$ and dry porous medium elasticity $\mathbb{C}^{\hom}$.

Copyright © 2013 Asociación Argentina de Mecánica Computacional http://www.amcaonline.org.ar

3 THE CASE OF A ROCK MEDIUM WITH SHORT PARALLEL JOINTS

3.1 Mori-Tanaka estimates

In this section, we consider situation of a rock with short joints (i.e., cracks with load transfer). From a geometrical viewpoint, the joints are represented by oblate spheroids with attached orthonormal frame $\left(\underline{t}, \underline{t}', \underline{n} \right)$ (see Fig. 3). The radius of the oblate is a and the half opening is c. The aspect ratio $X = c/a$ of such a penny-shaped crack is subjected to the condition $X \ll 1$. In the continuum micromechanics approach employed herein, a crack represents an inhomogeneity embedded within the rock matrix. The rock matrix stiffness and joint stiffness are assumed to take the following form

$$\mathbb{C}^s = 3k^s \mathbb{J} + 2\mu^s \mathbb{K} \qquad \underline{\underline{k}} = k_n \, \underline{n} \otimes \underline{n} + k_t \left(\underline{t} \otimes \underline{t} + \underline{t}' \otimes \underline{t}' \right) \tag{16}$$

where k^s is the bulk modulus and μ^s is the shear modulus of rock matrix, whereas k_n and k_t denote respectively the normal stiffness and shear stiffness of the joint. The fourth-order tensors $\mathbb{J}$ and $\mathbb{K}$ are defined as $\mathbb{J} = \frac{1}{3} \underline{\underline{1}} \otimes \underline{\underline{1}}$ and $\mathbb{K} = \mathbb{I} - \mathbb{J}$.

We consider the situation of a homogeneous rock with parallel cracks defined by the same radius a and crack aspect ratio X. The volume fraction of cracks present in the medium is denoted by f :

$$f = \frac{4}{3} \pi \varepsilon X \tag{17}$$

where $\varepsilon = \mathcal{N} a^2$ is the crack density parameter of the considered set of parallel cracks introduced by Budiansky and O'Connel (1976), $\mathcal{N}$ being the number of cracks by unit volume.

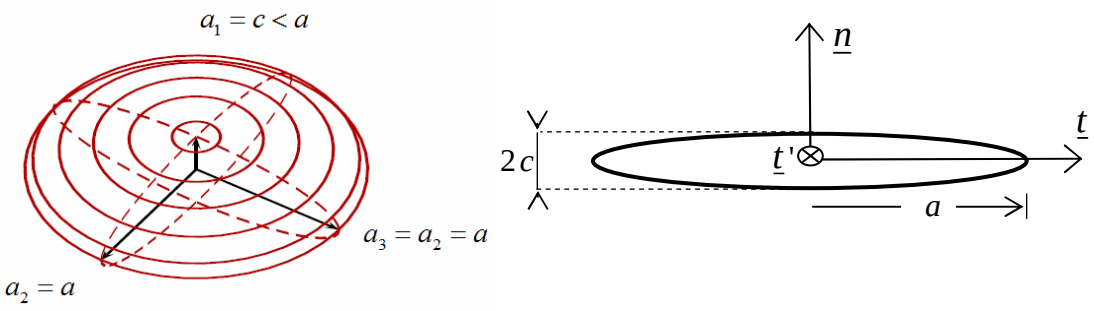

Figure 3: Joint as oblate spheroid.

Using a Mori-Tanaka scheme, the estimate of the tensor of drained moduli $\mathbb{C}^{\text{hom}}$ reads:

Copyright © 2013 Asociación Argentina de Mecánica Computacional http://www.amcaonline.org.ar

$$\mathbb{C}^{\hom} = \lim_{X\to 0} \left(\mathbb{c}^s + f\,\mathbb{c}^j : \left(\mathbb{I} + \mathbb{P} : (\mathbb{c}^s - \mathbb{c}^j) \right)^{-1} \right) : \left(\mathbb{I} + f \left(\mathbb{I} + \mathbb{P} : (\mathbb{c}^s - \mathbb{c}^j) \right)^{-1} \right)^{-1} \tag{18}$$

where $\mathbb{P} = \mathbb{P}(X, \underline{n})$ is the Hill tensor associated with the considered crack family. It depends on the aspect ratio X of the oblate spheroid and its orientation $\underline{n}$. The components of the Hill tensor of an oblate spheroid can be found in Handbooks (see for instance Nemat-Nasser and Horii 1993; Mura, 1997). Tensor $\mathbb{c}^j$ is related to the crack stiffness

$$\mathbb{c}^j = 3X\,a\left(k_n - 4/3k_t\right)\mathbb{J} + 2X\,a\,k_t\,\mathbb{K} \tag{19}$$

Assuming that all the joints have same poroelastic properties $\left(\underline{\underline{k}}, \alpha, m\right)$, the Mori-Tanaka estimate of the Biot tensor reads

$$\underline{\underline{B}} = \alpha \lim_{X\to 0} f\,\underline{\underline{1}} : \left(\mathbb{I} + \mathbb{P} : (\mathbb{c}^s - \mathbb{c}^j) \right)^{-1} : \left(\mathbb{I} + f \left(\mathbb{I} + \mathbb{P} : (\mathbb{c}^s - \mathbb{c}^j) \right)^{-1} \right)^{-1} \tag{20}$$

whereas the estimate of Biot modulus M is deduced from that of $\underline{\underline{B}}$ using (15).

The non-zero components of the Mori-Tanaka estimate of $\mathbb{C}^{\hom}$ are:

$$\begin{aligned}
C_{1111} &= C_{2222} = (3k^s + 4\mu^s)\,\frac{\kappa_2 + \pi(1+16/3\varepsilon)\,\kappa_1(1-\kappa_1)}{3\kappa_2 + 3\pi\,\kappa_1(1-\kappa_1) + 4\pi\varepsilon} \\
C_{3333} &= (3k^s + 4\mu^s)\,\frac{\kappa_2 + \pi\,\kappa_1(1-\kappa_1)}{3\kappa_2 + 3\pi\,\kappa_1(1-\kappa_1) + 4\pi\varepsilon} \\
C_{1122} &= C_{2211} = (3k^s - 2\mu^s)\,\frac{\kappa_2 + \pi(\kappa_1 + 8/3\varepsilon)(1-\kappa_1)}{3\kappa_2 + 3\pi\,\kappa_1(1-\kappa_1) + 4\pi\varepsilon} \\
C_{1133} &= C_{3322} = (3k^s - 2\mu^s)\,\frac{\kappa_2 + \pi\,\kappa_1(1-\kappa_1)}{3\kappa_2 + 3\pi\,\kappa_1(1-\kappa_1) + 4\pi\varepsilon} \\
C_{2323} &= C_{3131} = 2\mu^s\,\frac{4\kappa_3 + \pi\,(1-\kappa_1)(1+2\kappa_1)}{4\kappa_3 + 16/3\pi\varepsilon\,(1-\kappa_1) + \pi(1+2\kappa_1)(1-\kappa_1)} \quad ; \quad C_{1212} = \mu^s
\end{aligned} \tag{21}$$

where the non-dimensional parameters κ_1, κ_2 and κ_3 are defined by

$$\kappa_1 = \frac{3k^s + \mu^s}{3k^s + 4\mu^s} \quad ; \quad \kappa_2 = \frac{3k_n\,a}{3k^s + 4\mu^s} \quad ; \quad \kappa_3 = \frac{3k_t\,a}{3k^s + 4\mu^s} \quad ; \quad \kappa_4 = \frac{\mu^s}{3k^s + 4\mu^s} \tag{22}$$

The non-zero component of tensor $\underline{\underline{B}}$ are

$$B_{11} = B_{22} = 4\alpha\pi\varepsilon\,\frac{(4/3\kappa_1 - 1)\,\kappa_1 - 8/9(1-\kappa_1)^2}{3\kappa_2 + 3\pi\,\kappa_1(1-\kappa_1) + 4\pi\varepsilon} \quad ; \quad B_{33} = \frac{4\alpha\pi\varepsilon}{3\kappa_2 + 3\pi\,\kappa_1(1-\kappa_1) + 4\pi\varepsilon} \tag{23}$$

and the Biot modulus estimate can therefore be deduced from that of $\underline{\underline{B}}$

Copyright © 2013 Asociación Argentina de Mecánica Computacional http://www.amcaonline.org.ar

$$\frac{1}{M} = \frac{\pi / a}{m}\varepsilon + \alpha \, \underline{\underline{1}} : \left(\mathbb{C}^s\right)^{-1} : \underline{\underline{\underline{\underline{B}}}} \tag{24}$$

3.2 Comparison with finite element solutions in 2D setting

This section intends to assess the accuracy of the micromechanical predictions obtained in the case of parallel joints by comparison with finite element solutions based on the cohesive model (Needleman, 1987) that has been implemented in a simplified 2D-plane strain setting.

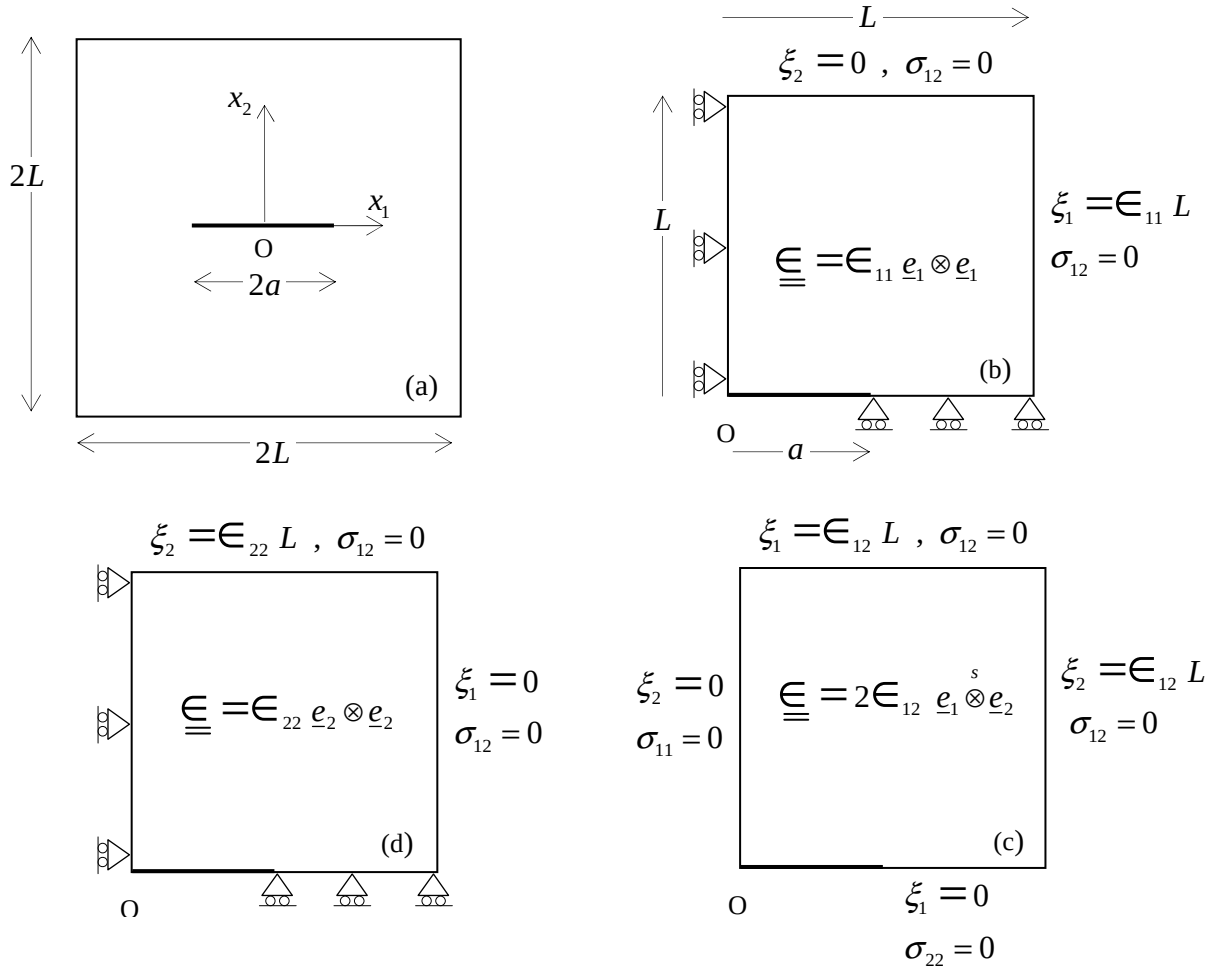

Figure 4: Geometry and loading of jointed medium: (a) elementary cell; (b) to (d) macroscopic strain states and associated boundary conditions.

We consider a simplified morphology for the jointed rock referring to a periodic distribution of joints. In the plane Ox_1x_2, the corresponding elementary cell (see Fig. 4a) is a square of side $2L$ with the rock matrix surrounding a central joint of length $2a$. The loading of the elementary cell is defined by three elementary macroscopic strain states: $\underline{\underline{\underline{\underline{E}}}} = \in_{11} \underline{e}_1 \otimes \underline{e}_1$, $\underline{\underline{\underline{\underline{E}}}} = \in_{22} \underline{e}_2 \otimes \underline{e}_2$ and $\underline{\underline{\underline{\underline{E}}}} = \in_{12} \left(\underline{e}_1 \otimes \underline{e}_2 + \underline{e}_2 \otimes \underline{e}_1\right)$. Owing to the periodicity

Copyright © 2013 Asociación Argentina de Mecánica Computacional http://www.amcaonline.org.ar

and symmetries of the problem, only a quarter of the elementary cell $\{x_1 \geq 0, x_2 \geq 0\}$ is considered, with the boundary conditions depicted in Figs. 4b, 4c and 4d (Suquet, 1987).

The rock matrix is modeled by standard 2D finite elements and the joint by cohesive elements. A regular mesh of the elementary cell consisting in 20×20 bilinear quadrangular elements is used for the numerical simulations. The joint is divided into linear cohesive elements of size $L/20$.

For comparison purposes, micromechanical predictions based on the Mori-Tanaka scheme have been derived representing each joint being by an infinitely long cylinder parallel to direction Ox_3 and having an elliptic cross-section in the plane Ox_1x_2 with vanishing aspect ratio.

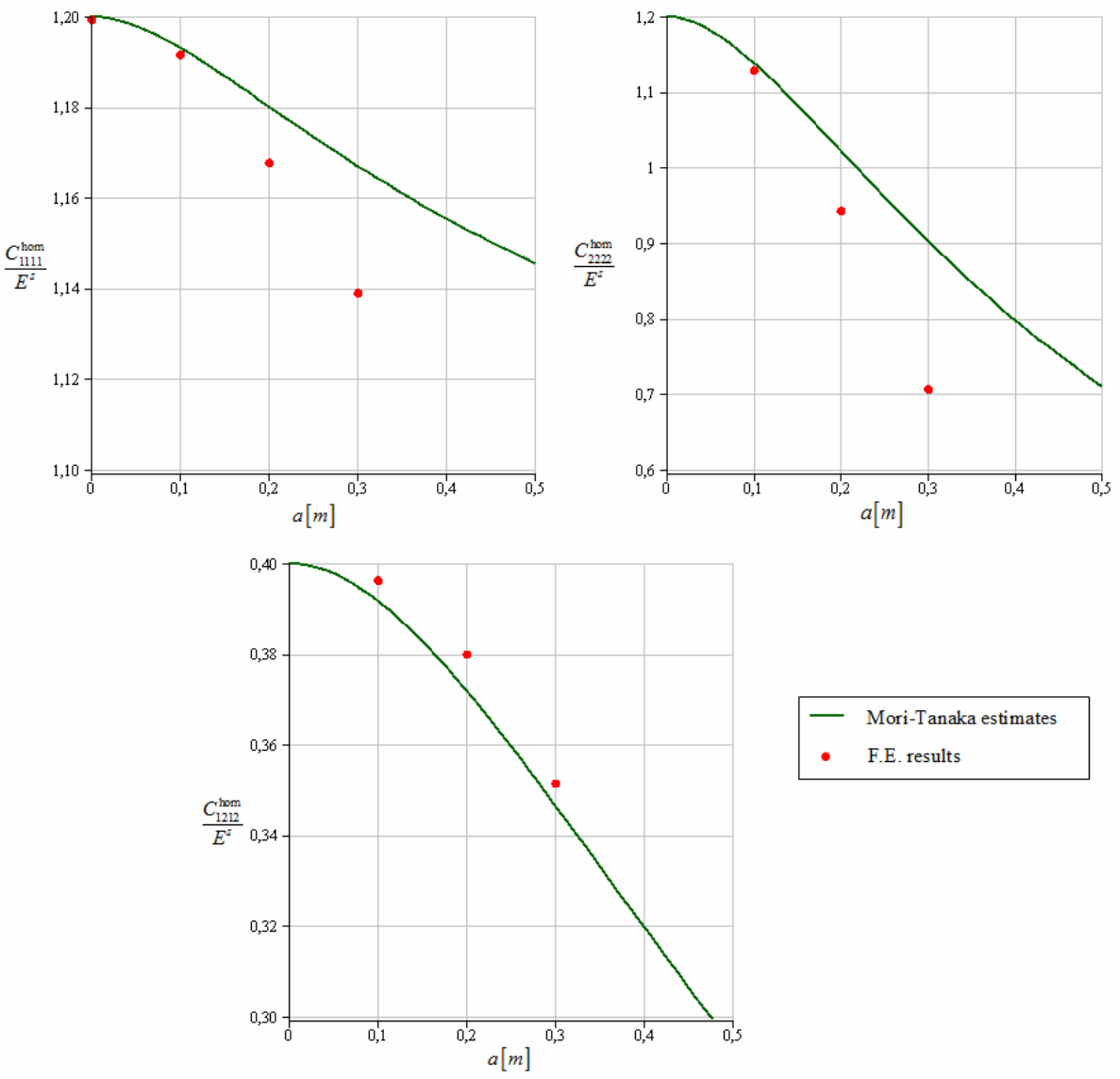

Figure 5: Effective elastic moduli of a rock with parallel joints as functions of joint length: Mori-Tanaka estimates versus finite element results.

Copyright © 2013 Asociación Argentina de Mecánica Computacional http://www.amcaonline.org.ar

The results of the finite element simulations together with the Mori-Tanaka estimates are plotted in Fig. 5. The numerical simulations have been performed considering the following model data: $L = 0.5m$, $a \in \{0.1m, 0.2m, 0.3m\}$, $\mathcal{N} = 1$, $k^s = 20GPa$, $\mu^s = 12GPa$, $k_n = 50GPa/m$, $k_t = 20GPa/m$. This preliminary analysis indicate that a good agreement between numerical simulations and the analytical estimates, more specifically for components C^{hom}_{1111} and C^{hom}_{1212}. For increasing joint length, the discrepancy observed for component C^{hom}_{2222} that stands for the elastic modulus in the direction orthogonal to joints suggests that the periodic morphology is no longer accurate to model randomly distributed parallel joints. In these figures, E^s denotes the Young modulus of rock matrix.

4 THE CASE OF A ROCK WITH ISOTROPIC DISTRIBUTION OF SHORT JOINTS

We consider now the case of a rock with randomly (isotropic) oriented short joints. Geometrically, the joints are represented by oblate spheroids with the same radius a and aspect ratio $X = c/a$. The orientation of each oblate inclusion in the 3D space is defined by two spherical angular coordinates $\theta \in [0, \pi]$ and $\varphi \in [0, 2\pi]$. Keeping the same notations as in section 3, the Mori-Tanaka estimate of macroscopic elastic tensor therefore reads

$$\mathbb{C}^{\text{hom}} = \lim_{X \to 0} \left(\mathbb{c}^s + \overline{\mathbb{c}^j : \left(\mathbb{I} + \mathbb{P} : (\mathbb{c}^s - \mathbb{c}^j) \right)^{-1}} \right) : \left(\mathbb{I} + \overline{\left(\mathbb{I} + \mathbb{P} : (\mathbb{c}^s - \mathbb{c}^j) \right)^{-1}} \right)^{-1} \tag{25}$$

where symbol $\overline{\mathcal{Q}}$ denotes the integral over the spherical angular coordinates $\theta \in [0, \pi]$ and $\varphi \in [0, 2\pi]$:

$$\overline{\mathcal{Q}} = \int_0^{\pi} d\theta \int_0^{2\pi} \frac{4\pi a^3}{3} X \; \mathcal{Q}(\theta, \varphi) \frac{\sin\theta}{4\pi} d\varphi \tag{26}$$

At the macroscopic level, the effective medium is elastically isotropic. Hence,

$$\mathbb{C}^{\text{hom}} = 3k^{\text{hom}} \mathbb{J} + 2\mu^{\text{hom}} \mathbb{K} \tag{27}$$

The homogenized bulk and shear drained moduli reads

$$k^{\text{hom}} = \frac{k^s}{1 + \dfrac{\frac{4}{3}\pi k^s / \mu^s}{\pi\kappa_1 + a k_n / \mu^s} \varepsilon} \; ; \; \mu^{\text{hom}} = \frac{\mu^s}{1 + \dfrac{6\kappa_2 + 4\kappa_3 + 9\pi\kappa_4 (3\kappa_1 + \kappa_4)}{15(3\pi\kappa_1\kappa_4 + \kappa_2)(4\kappa_3 + 9\pi\kappa_4(\kappa_1 + \kappa_4))} 16\pi\kappa_4 \varepsilon} \tag{28}$$

Copyright © 2013 Asociación Argentina de Mecánica Computacional http://www.amcaonline.org.ar

where parameters κ_1, κ_2, κ_3 and κ_4 are defined in (22).

The Biot tensor $\underline{\underline{B}} = b^{\text{hom}}\underline{\underline{1}}$ and Biot modulus read

$$b^{\text{hom}} = \frac{4\pi\alpha\varepsilon}{4\pi\varepsilon + 3\pi\kappa_1\mu^s/k^s + 4ak_n/k^s} \quad ; \quad \frac{1}{M} = \frac{\pi/a}{m}\varepsilon + \frac{4\pi\alpha^2\varepsilon}{4\pi k^s\varepsilon + 3\pi\kappa_1\mu^s + 4ak_n} \tag{25}$$

5 CONCLUSIONS

In the present paper, micromechanics-based poroelastic state equations for rocks with fluid saturated joint network have been derived. The formulation extends the classical mechanical model for microcracks to account for normal and tangential stresses across the joints. It has been proved that, provided the joints exhibit the same Biot coefficient, the determination of poroelastic properties reduces to that of drained elastic stiffness. The results are promising in view of numerical implementation in the context of a finite element tool devised for analyzing stresses and strains in jointed rock structures.

REFERENCES

Bandis, C.S., Lumsden, A.C., and Barton, N.R., Fundamentals of rock joint deformation. *Int. J. Rock Mech. Min. Sci. Geomech. Abstr.*, 20:249-268, 1983

Barton, N., Bandis, S., and Bakhtar, K., Stength, deformation and conductivity coupling of rock joints. *Int. J. Rock Mech. Min. Sci.*, 22:121-140, 1985.

Bart, M., Shao, J.F., Lydzba, D., and Haji-Sotoudeh, M., Coupled hydromechanical modeling of rock fractures under normal stress. *Canadian Geotech. J.*, 41:686-697, 2004

Goodman, R.E., *Methods of geological engineering in discontinuous rocks*, West Publishers, St Paul, 1976.

Boulon, M., Armand, G., Hoteit, N., and Divous, P., Experimental investigations and modeling of shearing of calcite healed discontinuities of granodiorite under typical stresses. *Engineering Geology*, 64:117-133, 2002.

Budiansky, B., and O'Connell, R.J., Elastic moduli of cracked solid. *Int. J. Solids Struc.*, 12:81-97, 1976.

Dormieux, L., Kondo, D., and Ulm, F.-J., *Microporomechanics*, Wiley, 2006

Indraratna, B., and Ranjith, P.G., *Hydromechanical aspects and unsaturated flow in jointed rock*, Balkema Publishers, Rotterdam, 2001.

Maghous, S., Bernaud, D., Fréard, J., and Garnier, D., Elastoplastic behavior of jointed rock masses as homogenized media and finite element analysis. *Int. J. Rock Mech. Min. Sci.*, 45:1273-1286, 2008.

Maghous, S., Dormieux, L., Kondo, D., and Shao, J.F., Micromechanics approach to poroelastic behavior of a jointed rock. *Int. J. Numer. Anal. Meth. Geomech.*, 37:111-129, 2013.

Mura, T., *Micromechanics of defects in solids. Martinus Nijhoff Publishers*, Dordrecht, 1987.

Needleman, A., Continuum model for void nucleation by inclusion debonding. *J. Appl. Mech.*, 54:525-531, 1987.

Nemat-Nasser, S., and Horii, H., *Micromechanics: overall properties of heterogeneous*

Copyright © 2013 Asociación Argentina de Mecánica Computacional http://www.amcaonline.org.ar

materials, North-Holland, Amsterdam, 1993.
Ng, K.L.A., and Small, J.C., Behavior of joints and interfaces subjected to water pressure. *Comput. Geotech.*, 20:71-93, 1997.
Nguyen, T.S., and Selvadurai, A.P.S., A model for coupled mechanical and hydromechanical behaviour of a rock joint. *Int. J. Numer. Anal. Meth. Geomech.*, 22:29-48, 1998.
Olsson, R., and Barton, N., An improved model for hydromechanical coupling during shearing of rock joints. *Int. J. Rock Mech. Min. Sci.*, 38:317-329, 2001.
Suquet, P., Elements of homogenization for inelastic solid mechanics. *In: Homogenization Techniques for Composite Media, Lecture notes in physics* 272, Springer, 193–278, 1987.
Zaoui, A., Continuum micromechanics: survey. *J. Eng. Mech. ASCE*, 128:808-816, 2002.

Copyright © 2013 Asociación Argentina de Mecánica Computacional http://www.amcaonline.org.ar